Effect of Surface Roughness on Propagation of Surface Plasmon Polaritons Along Thin Lossy Metal Films

Hoda Fadakar*, Abolghasem Zeidaabadi Nezhad**, and Amir Borji***
Department of Electrical and Computer Engineering, Isfahan University of Technology, Isfahan, IRAN
*h.fadakar@ec.iut.ac.ir, ** zeidabad@cc.iut.ac.ir, ***aborji@cc.iut.ac.ir

Abstract: *In this paper surface plasmon polaritons (SPP) that propagate along thin lossy metal films with surface irregularities are studied. Two cases of metal slab (with infinite width) and metal strip (with finite width) are considered. Surface roughness is modelled as a grating with deterministic profile. To analyze the slab structure the method of reduced Rayleigh equation is used. The results show that antisymmetric mode is strongly affected with roughness. Accuracy of the result is demonstrated through comparisons with HFSS simulations. The effect of surface roughness on the metal strip structure is only simulated by HFSS software. It shows that the attenuation of SPP modes is increased due to the surface roughness.*

Keywords: Surface plasmon polaritons (SPP), reduced Rayleigh equation, surface roughness

1. Introduction

Surface Plasmon Polaritons (SPP) are surface electromagnetic waves that are bound to the interface between two media where the real part of their permittivity have opposite signs. The field components of SPP decay exponentially away from the interface in transverse direction such that the lateral dimension of these waves is smaller than the free space wavelength. Therefore, plasmonic waveguides have attracted a lot of attention for applications in high density integration of optical components. Nobel metals such as gold and silver exhibit negative dielectric constant at visible and infrared wavelengths, thus propagation of bound waves at metal dielectric interface has been widely studied in recent years [1]-[3].

A metal film sandwiched between dielectric layers with infinite width (slab) and finite width (strip) as shown in Fig.1 is often used as plasmonic waveguide. This structure, with smooth surface, was analyzed by Berini with semi-analytical method of line [1]. Berini characterized the effects of varying width, thickness and background permittivity on dispersion of the purely bound modes that supported by these waveguides. One of the fundamental modes of these structures is a long range mode that has a long propagation length. The penetration depth of long range modes is less than penetration depth of short range ones so the attenuation due to absorption in the metal is reduced.

Tight confinement of the field to the metal surface makes SPP very sensitive to surface roughness. There are several studies on the effect of surface irregularities on the dispersion curve of SPP modes that propagate on the interface of lossless metal and dielectric [4]-[7]. In this paper we investigate the effect of surface roughness on the dispersion relation of SPP modes that propagate along a lossy metallic slab or strip. Surface roughness is modelled as a periodic grating with sinusoidal profile. In the case of slab waveguide the analytical method of reduced Rayleigh equation is used to obtain the dispersion curve of symmetric and antisymmetric modes. This structure is also simulated with HFSS eigensolver and the results are in close agreement with the analytical method.

For the metal strip waveguide there is no analytical solution, thus only the HFSS eigensolver is used.

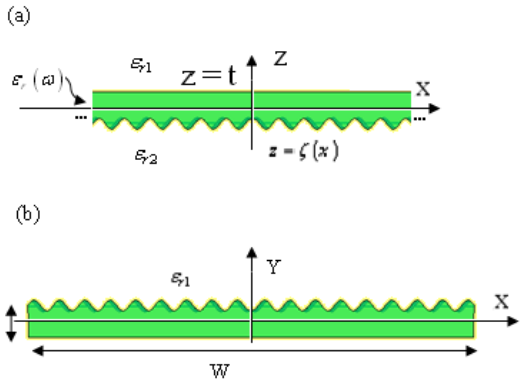

Figure 1: (a) metal slab waveguide (b) metal strip waveguide with one grating boundary

2. Slab waveguide

2.1 Theory

The structure is shown in Fig.1. It consists of a slab waveguide (dielectric /metal/ dielectric) that has two different interfaces: one of them is smooth (flat) and the contains a periodic grating whose profile is $\zeta(x)$. The thickness of the slab is t and its relative permittivity is $\varepsilon_r(\omega)$, surrounded by dielectric of relative permittivity

ε_{r1} and ε_{r2} . Only the SPP modes that propagate perpendicular to the grooves of grating (along x axis) are considered, so TM and TE polarizations are decoupled.

As it is well known, the infinitely wide symmetric structure supports only two bound TM surface modes with field components H_y , E_x and E_z . The components of the fields in the plane perpendicular to the direction of propagation have either symmetric or antisymmetric spatial distributions with respect to the Y axis. The symmetric mode has small attenuation constant but antisymmetric mode exhibits large attenuation because its field penetrates more into the metal [1]. According to [4] the magnetic field can be presented as:

for z>t

$$H_{y1}(x,z) = \sum_{m=-\infty}^{\infty} A_m(k\omega)\exp\left(jk_{xm}x - \alpha_m(k\omega)z\right) \quad (1)$$

for $z<\zeta(x)_{\min}$

$$H_{y2}(x,z) = \sum_{m=-\infty}^{\infty} D_m(k\omega)\exp\left(jk_{xm}x + \beta_m(k\omega)z\right) \quad (2)$$

for $\zeta(x)_{\max}$ <z<t

$$H_{y3}(x,z) = \sum_{m=-\infty}^{\infty}\exp\left(jk_{xm}x\right)\left[B_m(k\omega)\exp\left(-\gamma_m(k\omega)z\right) + C_m(k\omega)\exp\left(\gamma_m(k\omega)z\right)\right] \quad (3)$$

where $k_{xm} = k_x + 2\pi m / L$, $A_m(k\omega)$, $B_m(k\omega)$, $C_m(k\omega)$ and $D_m(k\omega)$ are Fourier coefficients and $\alpha_m(k\omega)$, $\beta_m(k\omega)$, $\gamma_m(k\omega)$ are defined as:

$$\alpha_m(k\omega) = \left(k_{xm}^2 - \varepsilon_{r1}k_0^2\right)^{1/2}$$

$$\beta_m(k\omega) = \left(k_{xm}^2 - \varepsilon_{r2}k_0^2\right)^{1/2}$$

$$\gamma_m(k\omega) = \left(k_{xm}^2 - \varepsilon_r(\omega)k_0^2\right)^{1/2} \quad (4)$$

with $\mathrm{Re}\{\phi_m(k\omega)\} > 0$, $\mathrm{Im}\{\phi_m(k\omega)\} < 0$ $\phi_m = \alpha_m, \beta_m, \gamma_m$.

After applying the boundary conditions and some manipulations the following equations are obtained [4]:

$$\begin{pmatrix} M_{nm}^{11} & M_{nm}^{12} \\ M_{nm}^{21} & M_{nm}^{22} \end{pmatrix}\begin{pmatrix} A_m \\ D_m \end{pmatrix} = 0, \quad \begin{matrix} \text{m= -N, -N-1,...N-1, N} \\ \text{n= -N, -N-1,...N-1, N} \end{matrix} \quad (5)$$

$$M_{nm}^{11} = \frac{\exp(-\alpha_m t)}{2}\left[J_{n-m}^{m}\exp(\gamma_m t)\left(1+\frac{\varepsilon_r(\omega)\alpha_m}{\varepsilon_{r1}\gamma_m}\right) + K_{n-m}^{m}\exp(-\gamma_m t)\left(1-\frac{\varepsilon_r(\omega)\alpha_m}{\varepsilon_{r1}\gamma_m}\right)\right] \quad (6)$$

$$M_{nm}^{12} = -L_{n-m}^{m} \quad (7)$$

$$M_{nm}^{21} = \frac{\exp(-\alpha_m t)}{2\varepsilon_r(\omega)\gamma_m}\left[-J_{n-m}^{m}\exp(\gamma_m t)\left(1+\frac{\varepsilon_r(\omega)\alpha_m}{\varepsilon_{r1}\gamma_m}\right) + K_{n-m}^{m}\exp(-\gamma_m t)\left(1-\frac{\varepsilon_r(\omega)\alpha_m}{\varepsilon_{r1}\gamma_m}\right)\left(k_{xm}k_{xn} - \varepsilon_r(\omega)k_0^2\right)\right] \quad (8)$$

$$M_{nm}^{22} = \frac{-L_{n-m}^{m}}{\varepsilon_{r2}\beta_m}\left(k_{xm}k_{xn} - \varepsilon_{r2}k_0^2\right) \quad (9)$$

Equation (5) is the so called reduced Rayleigh equation and Fourier coefficients in these equations are defined by:

$$J_r^{(m)}(k\omega) = \frac{1}{L}\int_0^L dx\,\exp\left(-j\frac{2\pi r}{L}x\right)\exp\left(-\gamma_m(k\omega)\zeta(x)\right)$$

$$K_r^{(m)}(k\omega) = \frac{1}{L}\int_0^L dx\,\exp\left(-j\frac{2\pi r}{L}x\right)\exp\left(\gamma_m(k\omega)\zeta(x)\right)$$

$$L_r^{(m)}(k\omega) = \frac{1}{L}\int_0^L dx\,\exp\left(-j\frac{2\pi r}{L}x\right)\exp\left(\beta_m(k\omega)\zeta(x)\right) \quad (10)$$

After truncating the Floquet modes to N , dimension of the matrix becomes $2(2N+1)\times 2(2N+1)$. The dispersion relation of SPP is obtained by equating the determinant of the coefficients A_m and D_m in (5) to zero. In this paper a sinusoidal profile function is considered, namely $\zeta(x) = \zeta_0\cos(2\pi x / L)$. Thus, the Fourier coefficients become modified Bessel's functions:

$$K_r^{(m)}(k\omega) = I_r(\gamma_m\zeta_0)$$

$$L_r^{(m)}(k\omega) = I_r(\beta_m\zeta_0)$$

$$J_r^{(m)}(k\omega) = (-1)^r I_r(\beta_m\zeta_0) \quad (11)$$

2.2 Numerical results

To verify the formulation, we also reproduce the results of a smooth slab ($\varepsilon_{r1} = \varepsilon_{r2}$ and $\zeta_0 = 0$) and compare our results with those of Berini which were obtained with a different method. The free space wavelength is set to $\lambda = 0.633\,\mu$m , the relative permittivity of the silver film at this wavelength is $\varepsilon_r(\omega) = -19 + j0.53$, and the permittivity of the surrounding media is assumed to be $\varepsilon_{r1} = \varepsilon_{r2} = 4$. The dispersion curve for a silver slab with $L = 50$ nm and different values of $\zeta_0 = 0, \zeta_0 = 0.1L, \zeta_0 = 0.2L$ were obtained. Figures 2 to 4 show the real and imaginary parts of k_x / k_0 as a function of slab thickness t for symmetric-like "s" and antisymmetric-like "a" modes. In order to achieve convergence, it is enough to choose $N = 4$. For $\zeta_0 = 0$ the surface becomes flat and the results are in good agreement with [1]. In [1] the problem is solved by method of line (MOL) which is an accurate semi analytical method. The attenuation of the "a" mode is increased with decreasing the thickness of the film because the fields penetrate more into the lossy silver

film. In the "s" mode with decreasing the thickness the attenuation is decreased and the mode evolves towards the TEM wave supported by the background. This mode is a long range SPP.

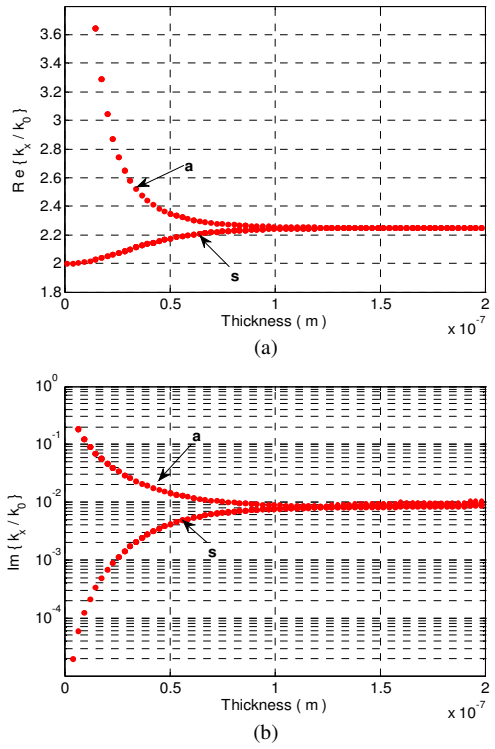

Figure 2: propagation constant k_x / k_0 in terms of silver slab thickness (a) real part (b) imaginary part for $\zeta_0 = 0$

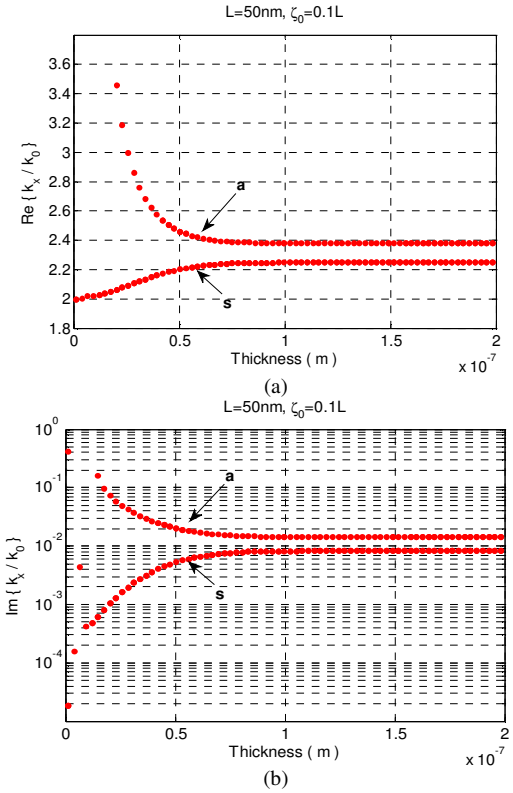

Figure 3: propagation constant k_x / k_0 in term of silver slab thickness (a) real part (b) imaginary part for $\zeta_0 = 0.1L$

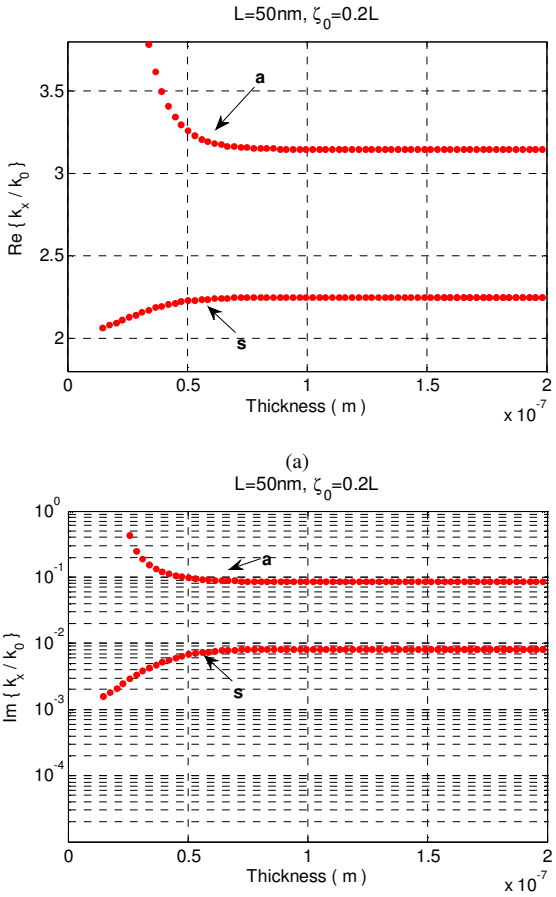

Figure 4: propagation constant k_x / k_0 in term of silver slab thickness (a) real part (b) imaginary part for $\zeta_0 = 0.2L$

In figures 3 and 4 it is observed that with increasing the depth of the grating (roughness) the real and imaginary parts of propagation constant k_x of "a" mode are increased. However, the overall behaviour of "s" and "a" modes do not change, *i.e.* with decreasing the thickness of the film, the attenuation of a mode is increased and that of the "s" mode is decreased. As the separation between the top and bottom interfaces increases, the "s" and "a" modes split into a pair of uncoupled SPP modes localized at the silver /dielectric interface. For the flat interface, $\zeta_0 = 0$, the "s" and "a" modes become degenerate but in the presence of surface roughness the degeneracy is broken such that the "s" mode converges to the SPP wave that propagates on a flat interface and the "a" mode converges to the SPP that propagates on a grating interface. When there is a grating in one side of the slab, the spatial distribution of the fields is not truly symmetric or antisymmetric about Y axis although they are localized near one of the interfaces. The "s" mode field distribution has a maximum at the flat interface while the "a" mode has a maximum at the grating interface. In the case $\zeta_0 \neq 0$ the "s" mode has a

cut-off thickness, because the mode cannot evolve into a TEM wave supported by the background.

For comparison, the metal slab with $\zeta_0 = 0.2L$ is also simulated with eigenvalue solver of HFSS software. Fig. 5 shows the magnitude of the electric field of "s" and "a" modes for $t = 0.06\ \mu$m. It is observed that the "a" mode fields are localized at the grating interface but the fields of "s" mode are localized at the flat interface therefore the propagation constant k_x of "a" mode is sensitive to the height of grating or surface roughness. Moreover, with increasing the slab thickness the propagation constant of "s" and "a" modes converge toward two different values.

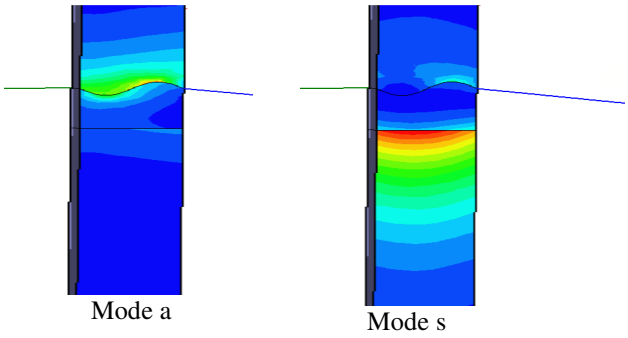

Figure 5: Magnitude of electric field of symmetric and antisymmetric modes

The dispersion curve that is obtained from HFSS simulation is shown in Fig.6. The results are in good agreement with results of reduced Rayleigh equation method.

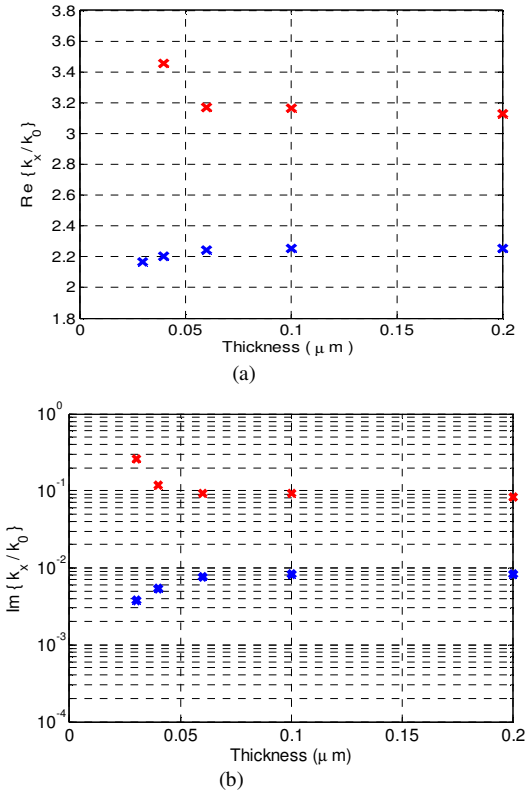

Figure 6: propagation constant k_x / k_0 in term of silver slab thickness (a) real part (b) imaginary part for $\zeta_0 = 0.2L$ using HFSS

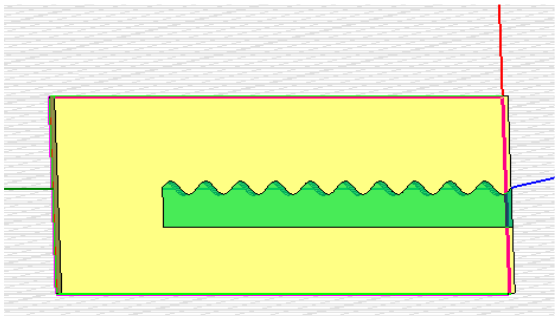

Figure 7: unit cell for simulating metal strip waveguide with one grating boundary

3. Strip waveguide

3.1 Numerical method implementation

There is no analytical method for the analysis of the effect of grating on the metal strip with finite width embedded in lossless dielectric material, so only HFSS is employed. With the use of eigensolver module in HFSS the real and imaginary parts of the propagation constant can be calculated [8].The method that is used in this paper differs slightly with [8]. In [8] the permittivity of lossy silver is function of frequency as determined by Johnson and Christy [9]. But in this simulation in order o remain consistent with Berini results, only a single frequency is considered $(\lambda = 0.633\ \mu\text{m})$, thus Silver is defined with permittivity $\varepsilon_r(\omega) = -19 + j0.53$ and dielectric host with constant permittivity $\varepsilon_{r1} = 4$. The structure is illustrated in Fig.1 (b), the symmetry can be used to reduce the computational domain, therefore, only half of the structure is analyzed as shown in Fig.7. In the direction of propagation the periodic boundary conditions are used. Periodic boundary condition ensures that the fields in the slave plane differ from the fields in the master plane within a phase delay φ so that the field components satisfy $g(z+d) = \exp(i\varphi)\, g(z)$ where d is the distance between the two planes. For each value of φ eigensolver provides a complex eigen frequency for each mode. The real part of the computed eigen frequency should be equal to frequency f_0 that corresponds to $\lambda = 0.633\ \mu$m. Therefore, we must sweep the value of φ and determine φ_0 that satisfies the above condition. Having determined φ_0, the real part of propagation constant can be found from $k_{zr} = \varphi_0 / d$. The imaginary part of propagation constant is calculated according to $k_{zi} = \text{Im}\{f_0\} / v_g$ where v_g is the group velocity given by $v_g = d(\text{Re}\{f\}) / dk_{zr}$. As mentioned in [3] d should be chosen sufficiently small for non-periodic problem so that the folded dispersion curve in the Brillouin zone boundary occurs at frequency beyond the spectral range that is considered. Careful review of the field distribution is generally required to identify the modes of interest that have their fields localized close to the metallic strip.

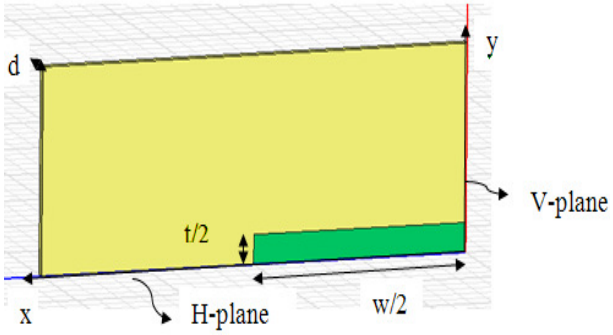

Figure 8: unit cell for simulating flat strip waveguide of Berini

3.2 Numerical results

To compare our results with [1] the flat silver strip is also simulated and some of the results reported by Berini in [1] are reproduced. The structure is shown in Fig.8. Utilizing the symmetry of the structure, only one quarter of the strip is simulated. The so called E or M symmetric boundaries in HFSS are used to obtain different modes of strip waveguide. The modes are divided into four categories depending on the symmetry of their fields and are labelled according to the nomenclature proposed by Berini. Therefore, a pair of letters is used to indicate that E_y is symmetric or antisymmetric with respect to vertical or horizontal plane, respectively. The superscript indicates the number of maxima of E_y along the larger dimension and when there is no maximum no superscript is used. Here only the bound mode is considered so the subscript b which means that the modes are bound to surface is eliminated. Simulation results for $W = 1\ \mu$m and $d = 0.02\ \mu$m are depicted in Fig. 9. In the region that thickness of the film is small $t < 0.04\ \mu$m the mode density becomes very large, with modes spaced closely in frequency thus identifying the solution of interest becomes difficult so the result is given for $t \geq 0.04\ \mu$m. The ss, aa, sa, and as modes are the fundamental modes supported by the structure. The results have good agreement with Berini's results. The fields related to the modes that are antisymmetric with respect to horizontal plane penetrate more into the lossy silver than symmetric modes, so these modes are highly attenuated.

Simulation results of the structure that is depicted in Fig.7 are shown in Fig.10. Parameters of the sinusoidal grating are $L = 50$ nm and $\zeta_0 = 0.2L$. Comparison of Fig.9 and Fig.10 shows that propagation constant of all six modes are increased due to the surface roughness. Imaginary parts of the propagation constant of these modes are also increased because of the grating on the metal strip. This means that with increasing roughness of the surface the bound SPP wave becomes leaky and attenuation is increased.

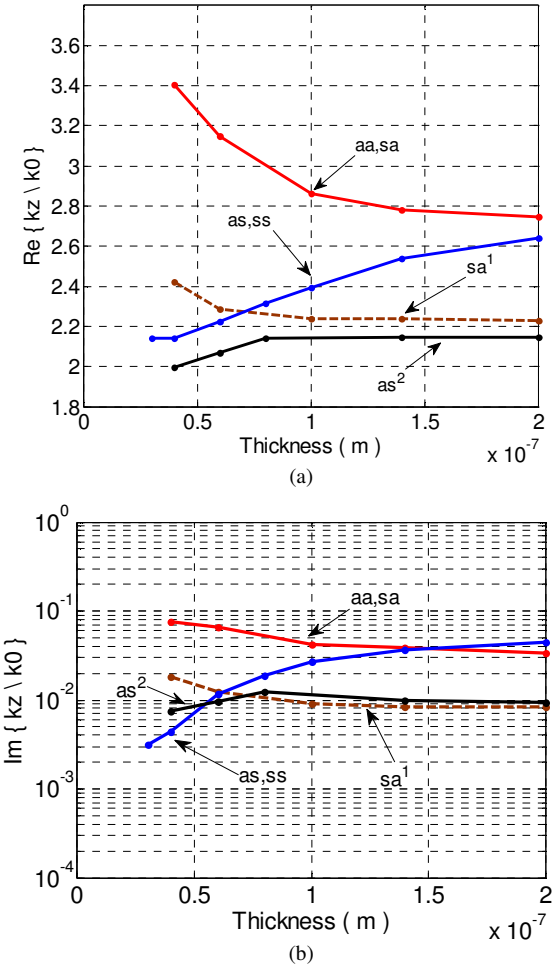

Figure 9: Simulation result of flat strip waveguide of Berini (a) real part (b) imaginary part of k_z / k_0

The field distribution of aa^2, sa^1 modes at $t = 0.14\ \mu$m is shown in Fig.11 and Fig.12. As mentioned in [1] the modes supported by a metal film of finite width are in fact super modes which are created from a coupling of edge and corner modes supported by each metal/dielectric interface defining the structure. In this structure, Because of the existence of grating on one interface, the supper modes may be created from the coupling of dissimilar interface modes. The coupled modes should have similar propagation constants and share the field symmetry with respect to the center vertical axis. In Fig. 11 for instance, it is seen that the grating edge mode has two exterma and is of higher order than the flat edge mode which has no extermum. In this structure, the grating interface has a higher phase constant than the flat interface. Because a supermode is created from a coupling of edge modes having similar propagation constants, it should be expected that in this structure different edge modes may couple to create a supermode. Higher-order modes have, in general, smaller values of phase constant compared to lower-order modes, so in this structure all supermodes are comprised of a grating edge mode of the same order or higher than the flat edge mode, as shown in Fig. 11 and Fig. 12.

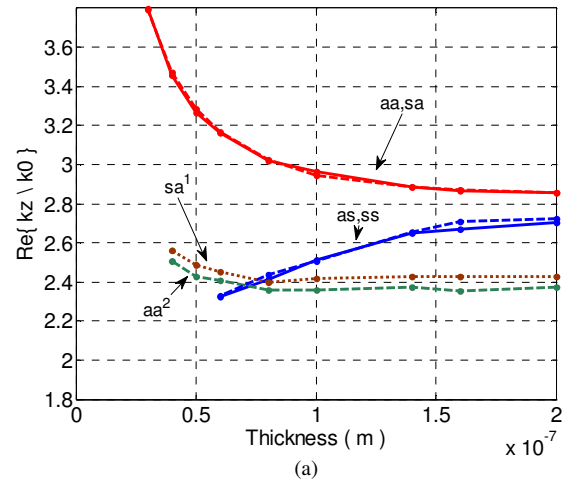

(a)

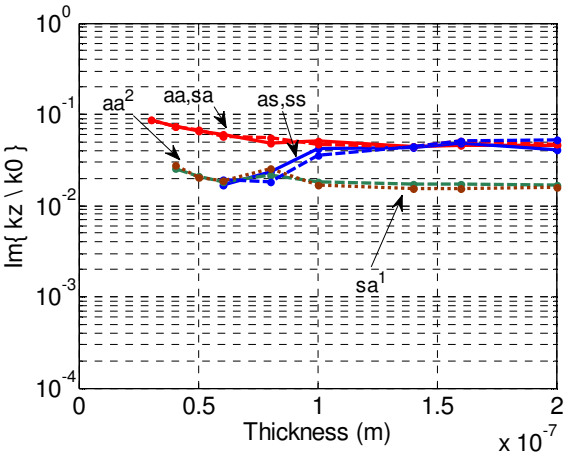

(b)

Figure 10: Simulation result of metal strip waveguide with one grating boundary (a) real part (b) imaginary part of k_z / k_0

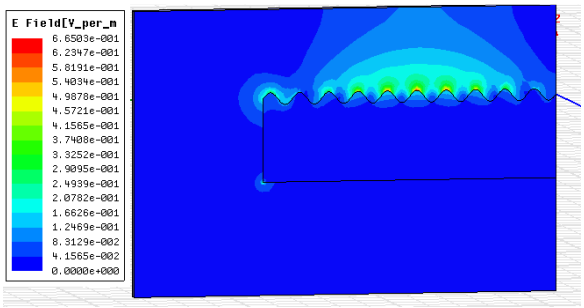

Figure 11: field distribution of aa^2 of grating strip with t = 0.14 μm

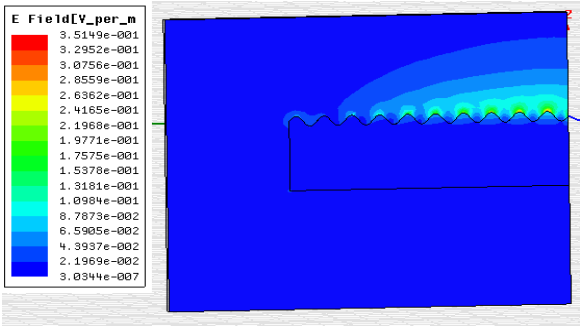

Figure 12: field distribution of sa^1 of grating strip with t = 0.14 μm

4. Conclusion

In this paper the effects of surface roughness on SPP waves that propagate on two structures, a lossy metallic slab and a lossy metal strip are investigated. The results show that the roughness that is modelled by a grating of sinusoidal profile affects the modes that are antisymmetric with respect to horizontal plane. The real and imaginary parts of the propagation constant of these modes increase which means increased attenuation due to the roughness. In the case of slab waveguide the results of reduced Rayleigh equation method are compatible with HFSS results.

References

[1] P. Berini, "Plasmon-polariton wave guided by a thin lossy metal film of finite width bounded mode of symmetric structures," *Phys. Rev. B*, vol. 61, No. 15, pp. 10484-10503, Apr. 2000.

[2] P. Berini, "Plasmon-polariton modes guided by a metal film of finite width bounded by different dielectrics," *Opt. Express*, vol. 7, No. 10, 6 Nov. 2000.

[3] P. Berini," Plasmon-polariton wave guided by a thin lossy metal film of finite width bounded mode of asymmetric structures," *Phys. Rev. B*, vol. 63, 13 Mar.2001.

[4] M. M. Auto, G. A. Farias, and A. A. Mardudin, "Surface polariton on metal films with grating surface," *Surface Science*, vol.167, No.1, pp. 57-69, March 1986.

[5] Bernardo Laks, D. L. Mills, and A. A. Maradudin, "Surface polariton on large-amplitude gratings," *Phys. Rev. B*, Vol. 23,No. 10, pp.4965-4976, May 1981.

[6] C. Kuo, and M. Moghaddam," A Theoretical Analysis of back scattering enhancement due to surface plasmons from multilayer structures with rough interfaces," *IEEE Trans. Antennas Propagat*, vol. 56, NO. 4, Apr. 2008.

[7] F. Toigo, A. Marvin, V. Celli, and N.R. Hill, "Optical properties of rough surfaces: General theory and small roughness limit," *Phys. Rev. B*, vol. 15, NO.12, Jun. 1977.

[8] A. Degiron, and D. R. Smith, "Numerical simulations of long-range plasmons," *Opt. Express*, vol. 14, No. 4,pp. 1611-1625, 2006

[9] P. B. Johnson, and R. W. Christy, "Optical Constants of the Noble Metals," *Phys. Rev. B,* vol. 6, No.12, pp. 4370-4379, Des. 1972.